

Conf - 930159 - -45

UCRL-JC-113277
PREPRINT

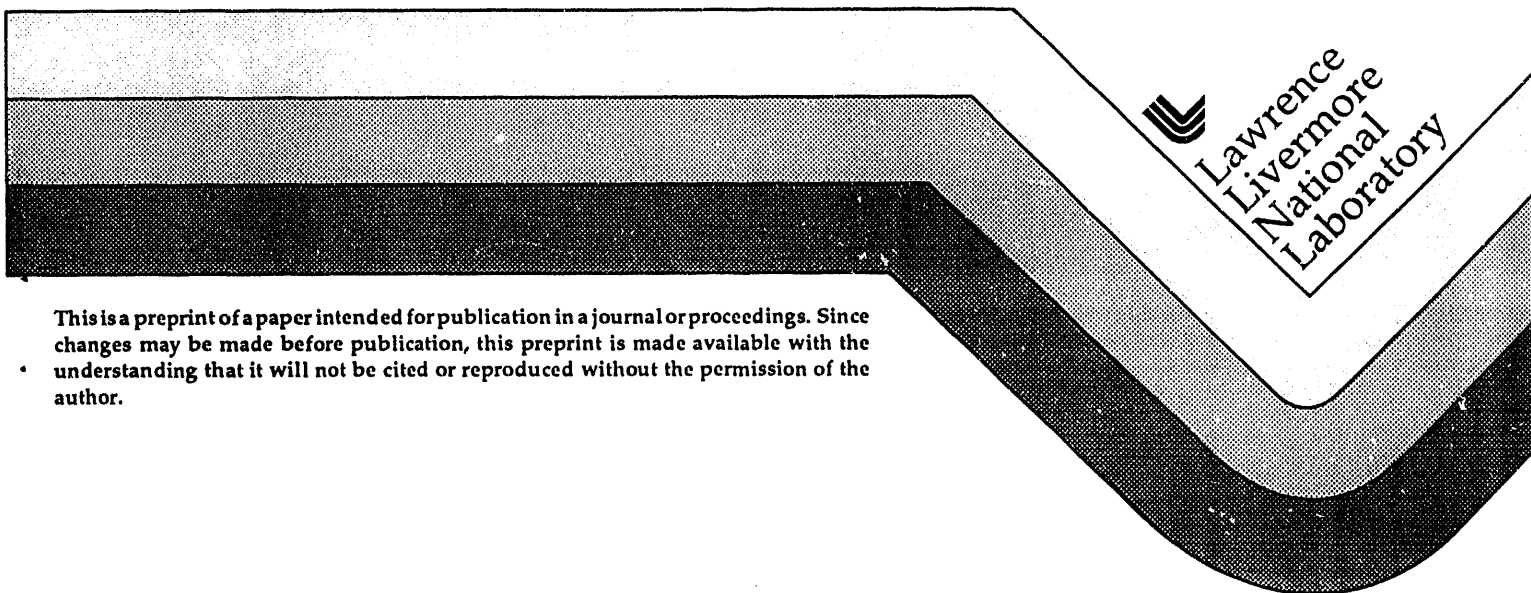
Observation of Nonsequential Ionization of Helium and
its Impact on Intensity Monitoring

RECEIVED
JUL 19 1993
OSTI

D. N. Fittinghoff, P. R. Bolton, B. Chang, and K. C. Kulander

This paper was prepared for submittal to the
Society of Photo-Optical Instrumentation Engineers Conference
Los Angeles, CA
January 16-23, 1993

March 19, 1993



Lawrence
Livermore
National
Laboratory

This is a preprint of a paper intended for publication in a journal or proceedings. Since changes may be made before publication, this preprint is made available with the understanding that it will not be cited or reproduced without the permission of the author.

DISCLAIMER

This document was prepared as an account of work sponsored by an agency of the United States Government. Neither the United States Government nor the University of California nor any of their employees, makes any warranty, express or implied, or assumes any legal liability or responsibility for the accuracy, completeness, or usefulness of any information, apparatus, product, or process disclosed, or represents that its use would not infringe privately owned rights. Reference herein to any specific commercial product, process, or service by trade name, trademark, manufacturer, or otherwise, does not necessarily constitute or imply its endorsement, recommendation, or favoring by the United States Government or the University of California. The views and opinions of authors expressed herein do not necessarily state or reflect those of the United States Government or the University of California, and shall not be used for advertising or product endorsement purposes.

Observation of nonsequential ionization of helium and its impact on intensity monitoring

D. N. Fittinghoff

UC Davis Dept. Applied Science/Livermore
Lawrence Livermore National Laboratory
Livermore, CA 94550

and

P. R. Bolton, B. Chang and K. C. Kulander

Lawrence Livermore National Laboratory
Livermore, CA 94550

ABSTRACT

We have measured the ion yields for helium and neon ionized by 120 femtosecond, 614 nanometer laser pulses with intensities up to 10^{16} watts per square centimeter. We have found that the He II and Ne II data exhibit features incompatible with standard nonresonant sequential ionization. These features reduce the usefulness of optical field ionization for monitoring laser intensity. For the experiment, we expect dynamic resonances to have little effect on the ionization, and we attribute the features to nonsequential ionization based on the simultaneous saturation of the features and the singly ionized charge states.

2. MONITORING INTENSITY BY OPTICAL FIELD IONIZATION

New developments in laser technology have made focused field amplitudes of 1 atomic unit or more (1 atomic unit of field = 5.14×10^9 volts per centimeter) and pulse lengths near 100 femtoseconds routinely available. Optical field ionization (OFI) offers a straight forward way of monitoring the intensity of such pulses—if the ionization is sequential and nonresonant. A complete understanding of field ionization is also fundamental to the study of plasmas produced by intense ultra-short laser pulses.

2.1 Optical Field or Tunneling Ionization

In the study of optical field ionization of atoms and ions, using ultra-short pulses with high intensity isolates field, or tunneling, ionization from conventional multiphoton ionization. The well-known Keldysh adiabaticity parameter¹ γ , distinguishes tunnel ionization from conventional multiphoton ionization. Tunneling dominates for the case:

$$\gamma = (E_{ion}/2U_p)^{1/2} \ll 1 \quad (1)$$

Here E_{ion} is the ionization potential of the atom or ion being ionized and U_p is the pondermotive potential from the laser field. While the condition $\gamma < 1$ does not strictly define the tunneling regime², tunneling models are generally predictive in this regime to within intensity uncertainties inherent in typical ultra-short pulse laser ionization experiments³⁻⁵. In this experiment γ varies from 0.4 to 1.0, and the ionization occurs by tunneling.

2.2 Sequential Ionization

In standard sequential ionization, the ionization proceeds sequentially with the most loosely bound electron ionizing from the ground state of the atom or ion followed by the ionization of next most loosely bound electron from the ground state of the surviving ion. The ionization obeys the rate equations:

MASTER

ep

$$\begin{aligned}
\frac{dp_0}{dt} &= -\Gamma_0 p_0 \\
\frac{dp_1}{dt} &= -\Gamma_1 p_1 + \Gamma_0 p_0 \\
\frac{dp_2}{dt} &= -\Gamma_2 p_2 + \Gamma_1 p_1 \\
&\dots \\
\frac{dp_n}{dt} &= +\Gamma_{n-1} p_{n-1}.
\end{aligned}
\tag{2}$$

Here p_i is the probability that the atom is in the i th charge state, and Γ_i is the atomic ionization rate. Figure 1 shows the ion yields predicted for 120 femtosecond hyperbolic-secant squared pulses for three different ionization models. For the calculations the Gaussian beam focus is $4.5\mu\text{m}$ full-width-at-half-maximum. The models used are a single-active-electron numerical solution to the Schrödinger equation (SAE)⁶, the simple tunneling model⁷ and the Ammosov, Delone and Krainov (ADK) model for tunneling in a complex atom^{8,9}. The similarity between the yields predicted by the three models is due to the sequential nature of the rate equations. Indeed for tunneling processes the shape of the ion yield curves is characteristic with an initially strong dependence on intensity rolling off with ionization saturation of the focal volume¹⁰. To within thirty percent uncertainty in intensity, which is within the uncertainty generally obtainable in short pulse experiments, the three models predict the same ion yields. Thus the appearance intensities are numerically well defined for the purpose of monitoring intensity.

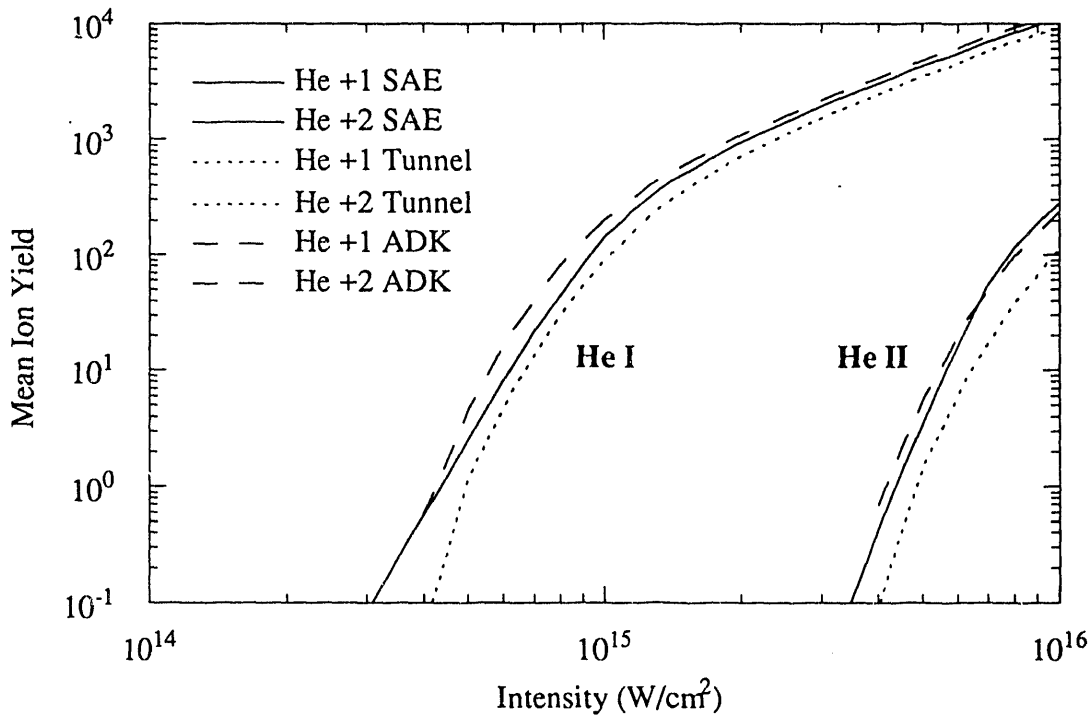


Figure 1. The predicted ion yields for three different ionization models. The differences in the yields are within the uncertainty in intensity for most ultra-short pulse experiments

2.3 Monitoring Scheme

Figure 2 illustrates the basic scheme for monitoring intensity by optical field ionization. The experimenter measures the number of ions, N_{ap} , produced for given laser conditions. The appearance intensity, I_{ap} , at which N_{ap} ions appear then sets

the intensity scale for the experiment. Using appearance intensity to monitor peak intensity has advantages. First, as noted before in Figure 1, for a given ion yield, the sequential ionization rate equations predict very similar intensities for many tunneling models. And second the appearance intensity of an ion is only a weak function of the appearance number chosen, of the pulse width and of the density. For the ADK model, the appearance intensity in atomic units for observing N_{ap} of the $k+1$ ion is

$$I_{ap}^{k+1} \approx \frac{4c}{9\pi} E_k^3 \left/ \left(\ln \left[K \frac{\tau \rho V_0 E_k}{N_{ap}} \right] \right)^2 \right. \quad (3)$$

E_k is the ionization potential of the k charge state, τ is the full-width-at-half-maximum pulse length, ρ is the initial atomic density, and K is a constant dependent on the initial quantum state of the electron. V_0 is the characteristic ionization volume for a Gaussian beam:

$$V_0 = \pi^2 w_0^4 / \lambda. \quad (4)$$

Here w_0 is the $1/e^2$ radius of the beam and λ is the wavelength. The appearance intensity depends on N_{ap} , τ and ρ only in the logarithm. This weak dependence makes the method for monitoring intensity easy to apply.

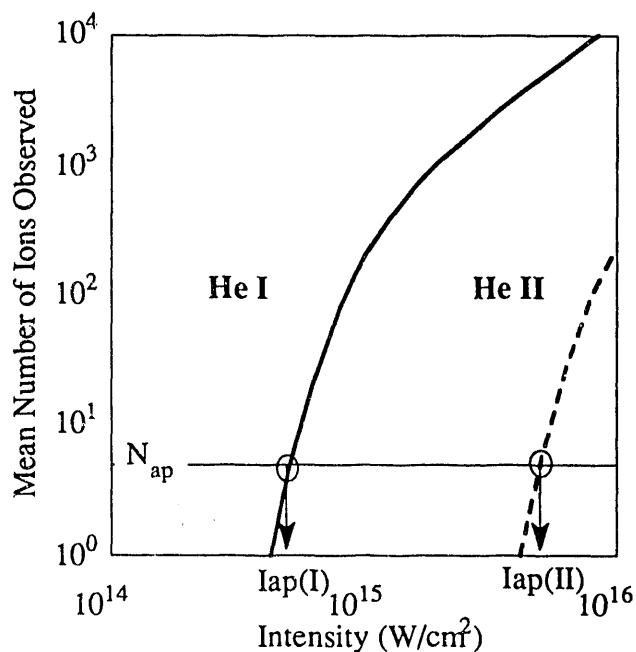


Figure 2 The intensity monitoring scheme relies on measuring the intensity at which a specific number, N_{ap} , of ions is detected.

3. EXPERIMENT

The laser used in this work is a colliding-pulse mode-locked dye laser that produces 2 millijoule pulses at 614 nanometers. An off-axis parabolic mirror focuses the beam to a 1.5 times diffraction limited full-width at half maximum of 4.5 micrometers. The energy of the laser pulse is measured on every laser shot using the reflection from a beam splitter, and single shot autocorrelations agree with a 120 femtosecond hyperbolic secant-squared temporal profile. We determine the intensity scale from the pulse energy, pulse width and numerical integration of the spatial profile at the focus. The absolute uncertainty in the intensity is a factor of 2. The ions produced in the focus are counted using a 1-meter ion time-of-flight tube with resolution sufficient to resolve doubly ionized helium and singly ionized molecular hydrogen. For each charge state, a computer bins and averages 8 to 12 thousand shots. The target gas pressures are from 10^{-3} to 10^{-5} Pa, and the background pressure is below 10^{-6} Pa

Figures 3 and 4 show the measured ion yields for helium and neon, respectively, plotted versus the measured intensity. The data is unshifted. The predictions of the ADK model are plotted for comparison. The agreement between the experiment and theory is excellent except for the lower intensity data for He II and Ne II which show strong ionization features incompatible with nonresonant sequential ionization. Insufficient data was obtained for Ne III, and the scatter in the data at the lower intensities makes identifying any feature uncertain. Using such data as a monitor of intensity is still possible; however the choice of N_{ap} is very important.

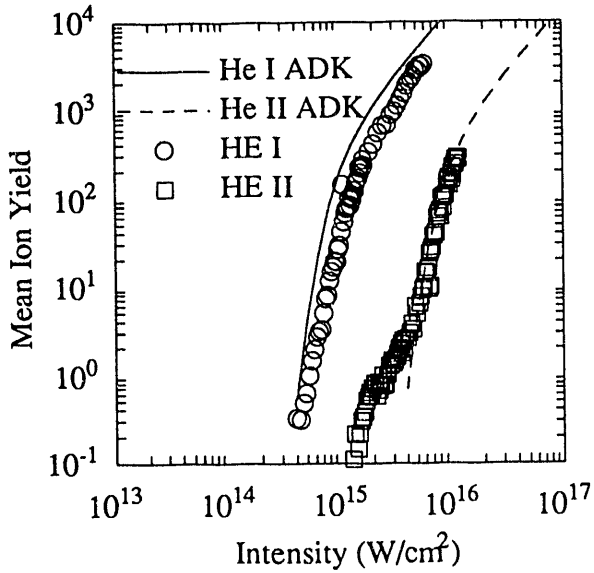


Figure 3. Measured ion yields for helium and the ADK theory predictions.

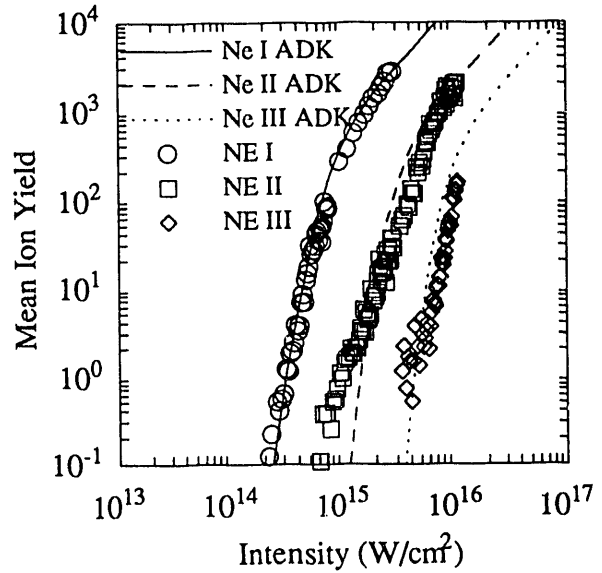


Figure 4. Measured ion yields for neon and the ADK theory predictions.

In Figure 5 we plot the ADK predictions for the appearance intensities versus the measured appearance intensities for $N_{ap}=15$. The solid line indicates exact agreement, and the dashed line indicates agreement with a factor of 1.2 shift down in the intensity scale of the data. The shift is within the 25 percent relative intensity uncertainty between charge states indicated by the error bars.

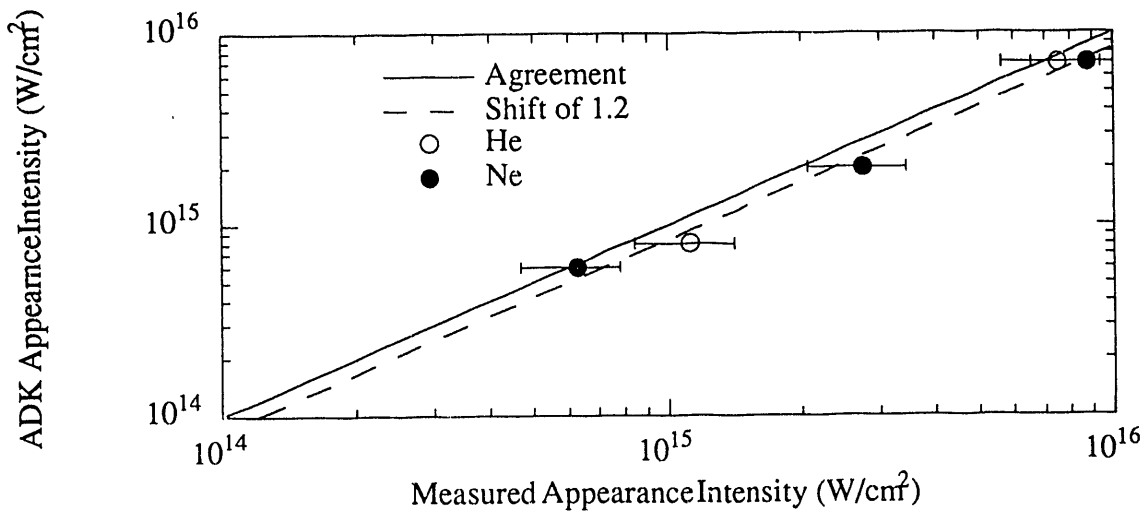


Figure 5. Plotting the ADK predictions for the 15 ion appearance intensity versus the measured 15 ion appearance intensity shows that an intensity scale may be set based on the optical field ionization data. Error bars indicate the 25% relative error. The absolute error is a factor of two.

Figures 6 and 7 show the data shifted down in intensity by a factor of 1.2 and the ADK model predictions. The agreement between the data and theory, excluding the features in He II and Ne II, is excellent. If the data were plotted versus pulse energy instead of intensity such a comparison between predicted appearance intensity and measured appearance energy would still find the intensity with reasonable accuracy. However, if such a comparison were based solely on the He II and Ne II yields below the 10 ion level, the intensity scale would be off by a factor of 2 to 3. Thus optical field ionization may be used to monitor intensity, but much more knowledge of the ionization is required than one predicts from the nonresonant sequential rate equations.

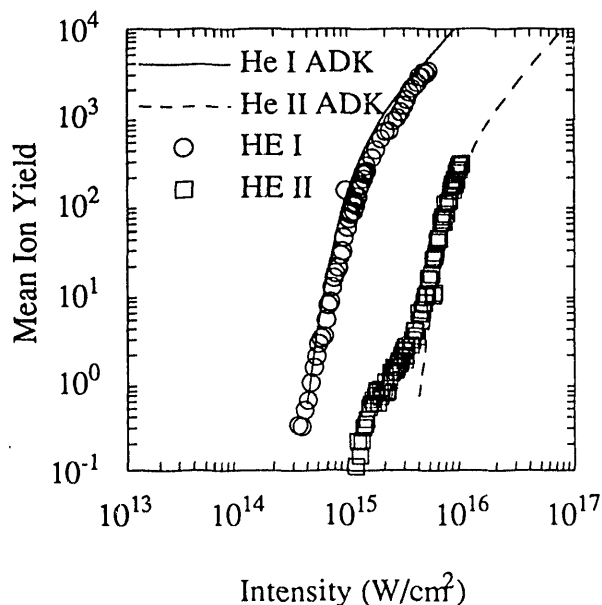


Figure 6 Measured ion yields for helium and the ADK theory predictions. The measured yields are shifted by a factor of 1.2 showing that an intensity scale may be determined based on the theoretical predictions.

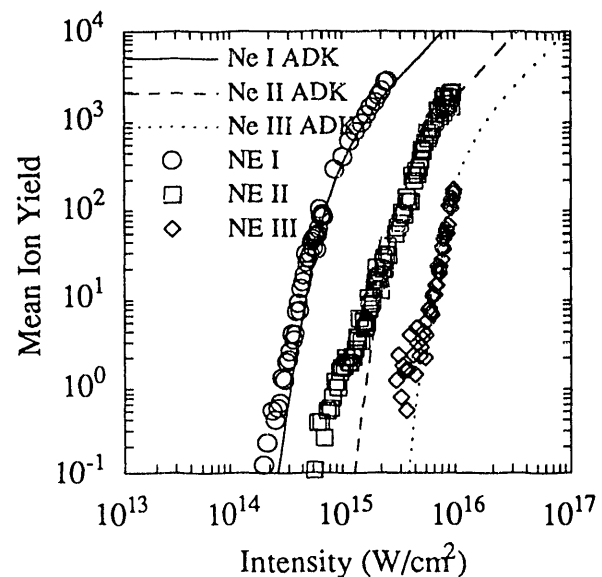


Figure 7 Measured ion yields for neon and the ADK theory predictions. The measured yields are shifted by a factor of 1.2 showing that an intensity scale may be determined based on the theoretical predictions.

4. RESONANCES

We are left with the question of what causes the features in the He II and Ne II ion yields. One possible explanation for the features is resonance effects. In the standard multiphoton ionization picture, if an energy level is dynamically shifted into resonance, the ionization rate increases which could result in the kinds of features observed¹¹. For this intensity and pulse width regime, we do not expect resonances to be important for several reasons. First, the ion yields for He II predicted by the SAE model show no evidence of any resonances. Since the SAE model is a numerical solution of the Schrödinger equation that treats one electron as active and the rest as an effective potential, the model should show any single electron resonances. Second, the double electron resonances in helium are 40 eV above the ionization potential and are unlikely to be the cause of the features. Finally, using the arguments of Chin et al.¹², we can calculate the dephasing time of a dynamic resonance. For this experiment, the resonance should dephase in less than 5 femtoseconds, and a resonance lasting less than three optical cycles should have little effect on the final ion yield.

5. NONSEQUENTIAL IONIZATION

In the data the feature in the He II ion yield saturates in parallel with He I ion yield. This is indicative of nonsequential ionization. In a previous paper¹³, we proposed a nonsequential mechanism to explain the discrepancy between the He II data and the sequential prediction. In this mechanism, the first electron leaves the atom so quickly, either by tunneling or over-

the-barrier escape, that the second electron has a substantial probability of being left in an excited state of the He I ion which is then immediately ionized. We implemented the mechanism in an ad hoc manner by modifying the rate equations to include a direct ionization channel that turns on at some critical intensity. We showed that a nonsequential term will reproduce the features with only one adjustable parameter. The idea of a direct process for ionization has also been proposed to explain data taken at longer pulse widths and different frequencies¹⁴⁻¹⁶. The model predicts that for helium the same critical intensity that produces an observable feature for 100 femtosecond pulses will make no observable difference in the ion yields for 1 picosecond pulses.

6. CONCLUSION

In conclusion, we have found enhancement features in the He II and Ne II ion yields. The features make monitoring laser intensity by optical field ionization more difficult than expected for nonresonant sequential ionization. The saturation in parallel of the He I ion yield and the feature in the He II ion yield and of the Ne I ion yield and the feature in the Ne II ion yield indicate that nonsequential ionization plays an important role in the ionization. A complete understanding of these effects will require more experiments studying the polarization dependence, electron energies and wavelength dependence. Understanding nonsequential effects may be critical for the study of plasmas produced by short pulse lasers.

7. ACKNOWLEDGMENTS

This work was performed under the auspices of the U.S. Department of Energy at Lawrence Livermore National Laboratory under contract number W-7405-Eng-48. We thank L. DiMauro and L. A. Lompré for enlightening discussions on nonsequential ionization.

8. REFERENCES

1. L. V. Keldysh, "Ionization in the field of a strong electromagnetic wave," *20*, 5 pp. 1307-1314 (1965).
2. B. E. Sauer, *et al.*, "Dynamic tunneling ionization of excited hydrogen atoms: a precise experiment versus theories," *Phys. Rev. Lett.* **68**, 4 pp. 468-471 (1992).
3. S. Augst, D. D. Meyerhofer, D. Strickland, and S. L. Chin, "Laser ionization of noble gases by Coulomb-barrier suppression," *J. Opt. Soc. Am. B* **8**, 4 pp. 858-867 (1991).
4. G. Gibson, T. S. Luk, and C. K. Rhodes, "Tunneling ionization in the multiphoton regime," *Phys. Rev. A* **41**, 9 pp. 5049-5052 (1990).
5. F. A. Ilkov, J. E. Decker, S. L. Chin, and N. B. Delone, "Ionization of atoms in the tunnelling regime with an experimental evidence using Hg Atoms," Centre D'optique, Photonique et Laser Département de Physique, Université Laval, Report No. 0953-4075, 1991.
6. J. L. Krause, K. J. Schafer, and K. C. Kulander, "High-order harmonic generation from atoms and ions in the high intensity regime," *Phys. Rev. Lett.* **68**, 24 pp. 3535-3538 (1992).
7. L. D. Landau and E. M. Lifshitz, *Quantum Mechanics Non-Relativistic Theory*, Pergamon, Oxford, 1965
8. A. M. Perelomov, V. S. Popov, and M. V. Terent'ev, "Ionization of atoms in an alternating electric field," *Sov. Phys. JETP* **23**, 5 pp. 924-934 (1966).
9. M. V. Ammosov, N. B. Delone, and V. P. Krainov, "Tunnel ionization of complex atoms and of atomic ions in an alternating electric field," *Sov. Phys. JETP* **64**, 6 pp. 1191-1194 (1986).
10. B. Chang, P. R. Bolton, and D. N. Fittinghoff, "Closed form solutions for the production of ions in the collisionless ionization of gases by intense lasers," *Phys. Rev. A*, (To be published).
11. M. D. Perry and O. L. Landen, "Resonantly enhanced multiphoton ionization of krypton and xenon with intense ultraviolet laser radiation," *Phys. Rev. A* **38**, 6 pp. 2815-2829 (1988).
12. S. L. Chin, C. Rolland, P. B. Corkum, and P. Kelly, "Multiphoton ionization of Xe and Kr with intense 0.62- μm femtosecond pulses," *Phys. Rev. Lett.* **61**, 2 pp. 153-156 (1988).

13. D. N. Fittinghoff, P. R. Bolton, B. Chang, and K. C. Kulander, "Observation of nonsequential double ionization of helium with optical tunneling," *Phys. Rev. Lett.* **62**, (1992).
14. A. l'Huillier, A. Lompre, G. Mainfray, and C. Manus, "Multiply charge ions induced by multiphoton absorption in rare gases at 0.53 μm ," *Phys. Rev. A* **27**, 5 pp. 2503-2512 (1983).
15. A. l'Huillier, L. A. Lompré, G. Mainfray, and C. Manus, "Multiply charged ions induced by multiphoton absorption processes in rare-gas atoms at 1.064 μm ," *J. Phys. B: At. Mol. Phys.* **16**, 1363-1381 (1983).
16. T. Auguste, P. Monot, L. A. Lompré, G. Mainfray, and C. Manus, "Multiply charge ions produced in noble gases by a 1 ps laser pulse at $\lambda=1053 \text{ nm}$," *J. Phys. B: At. Mol. Opt. Phys.* **25**, 4181-4194 (1992).

END

**DATE
FILMED**

8 / 18 / 93

